# News on Solar Neutrinos from Super-Kamiokande

Kunio Inoue
*Research Center for Neutrino Science, Tohoku University*
*Aramaki Aoba, Aoba, Sendai 980-8578, Japan*
E-mail: inoue@awa.tohoku.ac.jp

ABSTRACT

Solar neutrino results obtained from 708 days of Super-Kamiokande data are presented. D/N variation, seasonal variation and energy spectrum are measured in use of Super-Kamiokande's real-time and energy sensitive feature. Impacts of these measurements to the neutrino oscillation hypothesis is also discussed.

## 1. Introduction

Neutrino oscillation hypothesis [1,2] is the most popular way to explain the long-standing solar neutrino problem. Super-Kamiokande (SK) can play important roles in investigation of the various neutrino oscillation solutions, because SK has been an unique detector which can measure solar neutrinos in real-time and which can extract information of solar neutrino energy spectrum [3,4,5], except for the original Kamiokande detector [6]. SK is the ring imagining water Cherenkov detector filled with 50,000 tons of water and 32,000 tons of water is viewed by 11,146 PMTs which have photo-sensitive area of 20 inch in diameter. Fiducial volume for the solar neutrino observation is limited at 22,500 tons out of 32,000 tons inner volume, thus 2 meter from the PMT surface are not used for the measurement. SK utilizes a neutrino-electron elastic scattering and the strong forward peak of the scattering guarantee the excess is certainly coming from the Sun. Observed angular distribution toward the Sun with events above 6.5 MeV is shown in figure 1 and the number of excess toward the Sun is $9531^{+167}_{-155}$ events. This high statistics data is used for the $^8B$ solar neutrino flux measurement and investigation of time variations. And notably, SK has succeeded to lower the analysis threshold down to 5.5 MeV. This super-low energy (SLE) data has been accumulated for 419 days. Direction distribution of the SLE data is also shown in figure 1. We see clear excesses to the Sun and number of excess events are $1053^{+95}_{-85}$ and $858^{+64}_{-61}$ events for 5.5-6.0 MeV and 6.0-6.5 MeV, respectively. Spectrum measurement includes this SLE data so that the increased lever-arm improves a sensitivity to any possible spectrum distortion due to the various neutrino oscillation solutions.

## 2. $^8B$ solar neutrino flux

SK has started taking data in Apr $1^{st}$, 1996 as scheduled. But, a quality of the water, especially transparency, was not satisfactory for a solar neutrino observation at the very beginning. Solar neutrino sample covers the data from May $31^{st}$, 1996

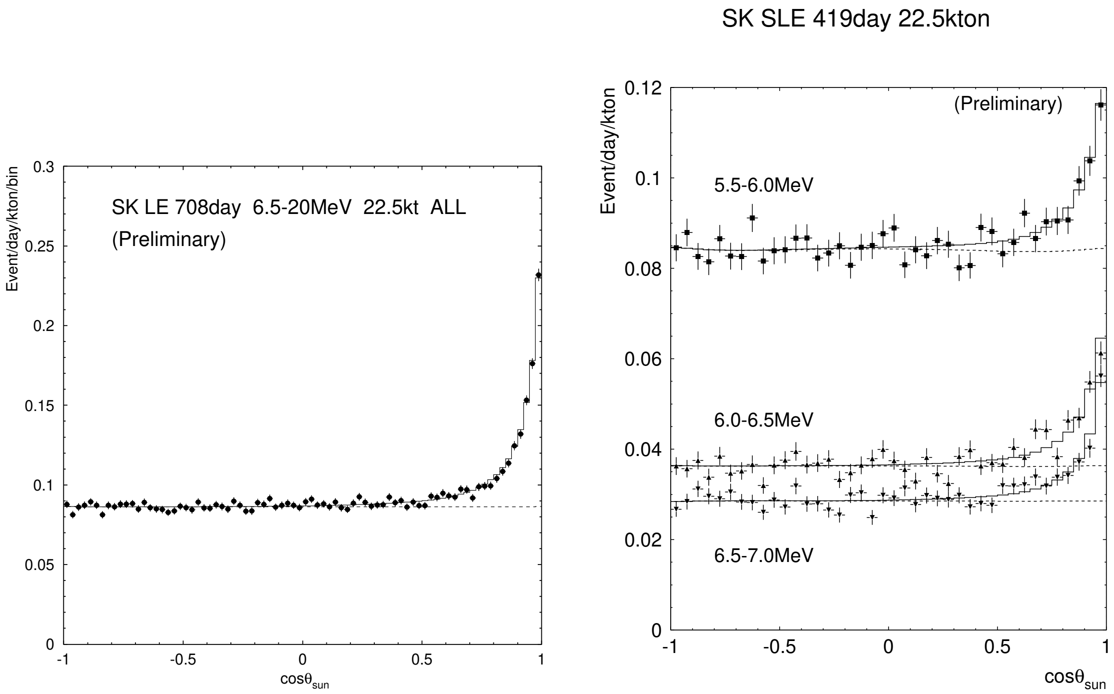


Figure 1: Angular distribution toward the Sun. Left side is for the events above 6.5 MeV and right side is for the SLE data.

after the transparency became stable. In this report, SK data up to Nov $4^{th}$, 1998 is used for the analysis and the total live time is 708 days. Full detector simulation which is precisely tuned with LINAC calibrations [7)] has been performed even tracing the change of the water transparency seen in SK water. Due to the accurate energy calibration by the LINAC system and the precisely tuned simulation, systematic errors from energy scale and direction uncertainties have been shrunk significantly as shown in Table.1. By comparing the angular distribution to the Sun with the expected distribution from the MC, the excess toward the Sun, $9531^{+167}_{-155}$ events, is interpreted as;

$$\Phi(^8B) = 2.419^{+0.042}_{-0.039}(stat)^{+0.068}_{-0.065}(sys) \times 10^6/cm^2/s$$

and the ratio of the flux to the standard solar models (SSM) [8,9)] are obtained as;

$$\frac{data}{SSM_{BP98}} = 0.470 \pm 0.008(stat) \pm 0.013(sys)$$

$$\frac{data}{SSM_{BTCM98}} = 0.502 \pm 0.008(stat) \pm 0.014(sys)$$

for the events above 6.5 MeV. The impact of this latest result is investigated in two active neutrino oscillation hypothesis combining with the results from Homestake

$(2.56 \pm 0.16 \pm 0.16 SNU)$ [10], SAGE $(66.6^{+7.8}_{-8.1} SNU)$ [11] and Gallex $(77.5 \pm 6.2^{+4.3}_{-4.7} SNU)$ [12]. The global analysis follows the method given in [13] with updated theoretical uncertainties [14,15,16]. Allowed regions are shown in figure 2 and four types of solutions (SMA, LMA, LOW and Justso) are found. The best fit parameter is obtained at $(6.3 \times 10^{-3}, 5.0 \times 10^{-6} eV^2)$ with the minimum $\chi^2$ value 0.9. The $\chi^2$ value for the no oscillation is 62.0 and the oscillation solution is strongly favored.

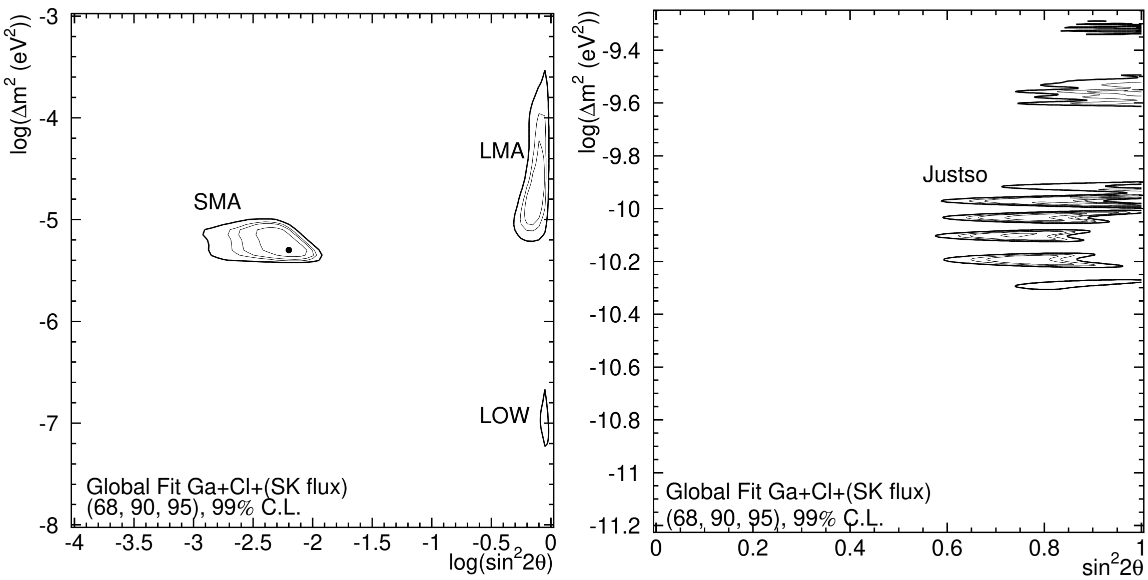


Figure 2: Allowed region from the global analysis. Homestake, SAGE, Gallex and SK flux results are used.

## 3. D/N variation

In some regions of the parameter space for the neutrino oscillation, matter enhanced oscillations within the Earth [17,18] can lead to a regeneration of the measured neutrino passing through the Earth. This regeneration would produce a higher flux measured during night time relative to day time measurements. If such a day-night (DN) variation was observed, it would be strong evidence for neutrino oscillations. The amplitude of the DN flux variation would determine the neutrino oscillation parameters, independent of the absolute flux uncertainties of the SSMs.

Figure 3 shows the observed DN fluxes and also shown are the expected variations with typical parameters in SMA $(0.01, 6.3 \times 10^{-6} eV^2)$ and in LMA $(0.56, 1.2 \times 10^{-5} eV^2)$. Expected regeneration effect around LMA is a flat enhancement in night time and an effect around SMA is a N5 excess when neutrinos penetrate the core of the Earth. These effects are tested by the following measures.

$$\frac{N}{D} - 1 = 0.060 \pm 0.036(stat) \pm 0.008(sys)$$

Table 1: Systematic errors: Systematic errors for the flux, seasonal and DN variation measurement with 6.5 MeV energy threshold is shown in percent. Errors for the flux is absolute but others are relative errors. () shows errors assigned in an old 504 days analysis.

| | Flux | Seasonal | DN |
|---|---|---|---|
| E-scale, Resolution | ${}^{+1.4}_{-1.5}$ ${}^{(+2.2)}_{(-1.1)}$ | ${}^{+1.2}_{-1.1}$ | ${}^{+1.2}_{-1.1}$ |
| $^8B$ spectrum | ${}^{+1.2}_{-0.9}$ ${}^{(+1.2)}_{(-1.1)}$ | — | — |
| Trigger efficiency | $\pm0.2$ | $\pm0.2$ | - |
| Noise event cut | $\pm0.7$ | - | - |
| Reduction | $\pm0.2$ | - | $\pm0.1$ |
| Vertex shift | $\pm1.5(\pm1.3)$ | - | - |
| non-flat B.G. | $\pm0.1$ | $\pm0.1$ | $\pm0.4$ |
| Direction | $\pm1.0(\pm2.2)$ | - | - |
| Cross section | $\pm0.5$ | - | - |
| Spallation dead time | $\pm0.1(\pm0.2)$ | $\pm0.1(\pm0.6)$ | $\pm0.1(\pm0.6)$ |
| Live time | $\pm0.1$ | $\pm0.1$ | $\pm0.1$ |
| Total | ${}^{+2.8}_{-2.7}$ ${}^{(+3.5)}_{(-2.9)}$ | ${}^{+1.2}_{-1.1}$ ${}^{(+1.4)}_{(-1.3)}$ | ${}^{+1.3}_{-1.2}$ ${}^{(+1.4)}_{(-1.3)}$ (binned)<br>${}^{+0.6}_{-0.5}$ (D,N combined) |

$$\frac{N5}{< others >} - 1 = -0.013^{+0.060}_{-0.058}(stat) \pm 0.013(sys)$$

N5 excess is not seen and the excess in night-time is not significant as the typical parameter shown in the figure 3. And two typical parameters shown in the figure are excluded. However a small excess in night time at 1.6 $\sigma$ level gives the best fit parameter at $(1.0, 2.0 \times 10^{-5} eV^2)$ near LMA solution. The expected variation with the parameter is also shown in the figure 3. The $\chi^2$ value of the best-fit parameter is 3.5 with 5 d.o.f. and that of no oscillation is 6.7, where $\chi^2$ is defined as;

$$\chi^2_{DN} = \min_{\alpha} \left[ \sum_{i=D,N_1,\cdots,n_5} \left\{ \frac{\phi_i - \alpha \times \phi_i^{osci}(\sin^2 2\theta, \Delta m^2)}{\sqrt{\sigma_i^2 + \sigma_{sys,i}^2}} \right\}^2 \right]$$

Thus, no oscillation is allowed at 80% C.L. but an excluded region is set with the DN information as shown also in the figure 3. In this analysis, absolute normalization is treated as free parameter making the results free from an absolute flux uncertainty of the SSMs. This excluded region scrapes high mixing part of SMA and limit the

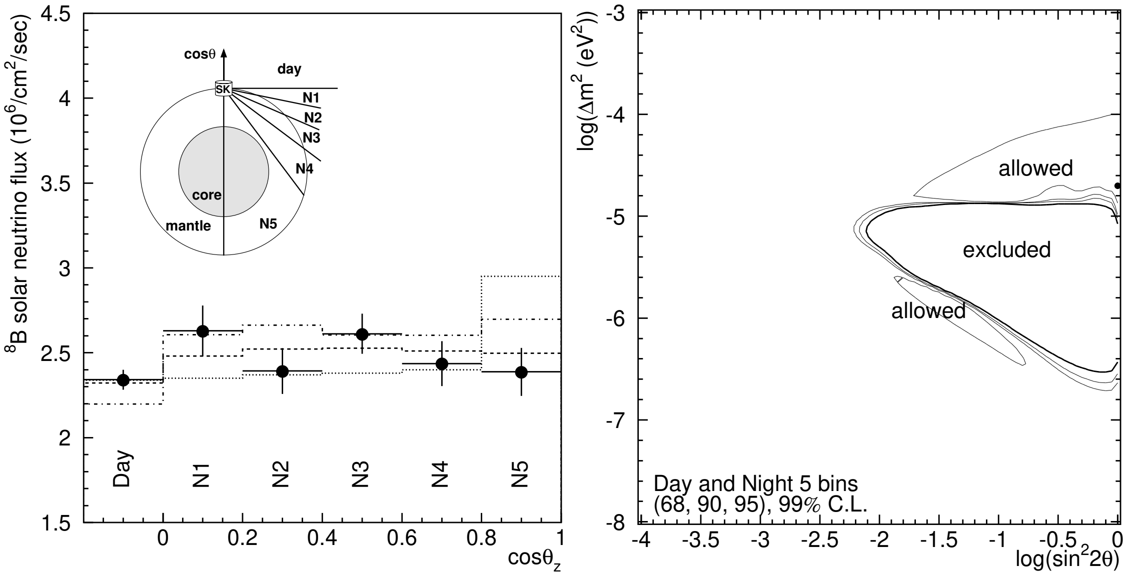


Figure 3: Left: Measured DN fluxes as a function of the nadir of the Sun. Error bars represent statistical error only. Night data is divided into 5 bins. Dotted histogram is the expected variation of a typical SMA solution $(0.01, 6.3 \times 10^{-6})$, and dot-dashes is that of a typical LMA solution $(0.56, 1.2 \times 10^{-5})$, and dashes is the best fit parameter $(1.0, 2.0 \times 10^{-5})$ $\chi^2 = 3.5$. Right: Allowed regions from DN variation are shown at 68, 90, 95 and 99% C.L..

mass difference of LMA solution to larger than $10^{-5}eV^2$.

## 4. Energy spectrum

SK observes recoil of electrons by solar neutrinos and doesn't measure neutrino energies directly. However, a significant distortion of neutrino energy spectrum makes electron spectrum different from the expectation of the standard model. SK has been calibrated with LINAC system and its precisely measured energy response allows us to distinguish tiny distortion of recoil electron energy spectrum from that of no oscillation. SSM prediction gives a negligible event rate of hep neutrinos which has the highest end point energy of 18.8 MeV and dominant solar neutrino events in SK is coming from $^8B$ neutrinos which has an end point energy of 15 MeV. However the uncertainty of the hep flux is not specified in the SSM and it can be significant in high energies if the flux is 10 times of the SSM prediction. Newly added SLE data since May 1997 has improved the sensitivity of SK to the spectrum distortion in the point of lever-arm of slope and even in the point of independence of the low energy results on the hep flux uncertainty. SLE data requires tighter reduction than a normal analysis in order to enhance a signal to noise ratio. All the data are processed with SLE reduction and the obtained results above 6.5 MeV were compared with those of the normal analysis. They agreed very well and the fact gave relative systematic error between the data below 6.5 MeV and that above 6.5 MeV to be less than 2%. The combined results (SLE analysis for below 6.5 MeV and normal analysis for above 6.5 MeV) are shown in figure 4. Also shown are the expected distortions of energy spectrum from the typical SMA solution by solid $(6.3 \times 10^{-3}, 5.0 \times 10^{-6} eV^2)$ and justso solutions by dots (justso1) $(0.80, 4.3 \times 10^{-10} eV^2)$ and by dashes (justso2) $(0.83, 7.1 \times 10^{-11} eV^2)$. In the figure, $^8B$ flux is treated as free but hep flux is fixed at the SSM value. A distortion of the spectrum can be made by adding extra hep flux in the calculation. The best fit spectrum with free hep flux but no oscillation is also shown in the figure by thick solid. The best fit was met at 14 times hep flux than the SSM prediction.

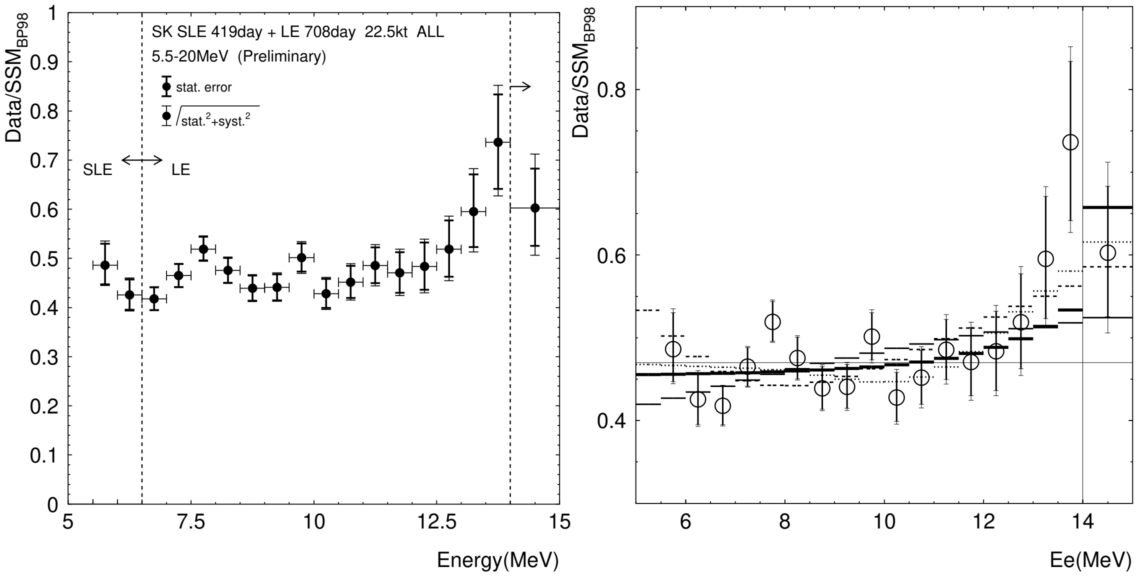


Figure 4: Left: Measured recoil electron energy spectrum is shown as ratios to the SSM prediction. Right: Expected spectra from typical SMA (solid), justso (dots and dashes) are shown together with the flat (thin solid) and 14 times hep with no oscillation (thick solid).

The fitness of the various expected distortions were tested by the following $\chi^2$.

$$\chi^2_{spec} = \min_{\alpha,\epsilon_{exp},\epsilon_{theo}} \left[ \sum_{i=1,18} \left\{ \frac{\phi_i - \phi_i^{osci} \times \alpha \times f_i(\epsilon_{exp}, \epsilon_{theo})}{\sqrt{\sigma^2_{stat,i} + \sigma^2_{uncorr.sys,i}}} \right\}^2 + \left( \frac{\epsilon_{exp}}{\sigma_{exp}} \right)^2 + \left( \frac{\epsilon_{theo}}{\sigma_{theo}} \right)^2 \right]$$

where $f_i(\epsilon_{exp}, \epsilon_{theo})$ is response function managing correlated errors coming from the uncertainty of energy scale, energy resolution (represented by $\sigma_{exp}$) and the uncertainty of $^8B$ neutrino spectrum [19] (represented by $\sigma_{theo}$). The obtained $\chi^2$ values are 27.4, 18.9, 28.3 and 26.8 for the typical SMA (solid), justso1 (dots), justso2 (dashes) and flat (thin solid). For obtaining the best fit hep flux, $\phi_i^{osci} \times \alpha$ is replaced by $\phi_{^8B,i} \times \alpha_{^8B} + \phi_{hep,i} \times \alpha_{hep}$ and both $\alpha_{^8B}$ and $\alpha_{hep}$ were iterated to meet the minimum $\chi^2$ which was 21.9 when $\alpha_{hep} = 14$. The justso1 parameter gives the best fit of spectrum shape and 14 hep also agrees with the measurement well. The typical SMA, justso2 and flat don't fit well and SLE data region looks promising to discriminate these spectra in near future.

In order to be independent of theoretical flux uncertainties and in order to extract oscillation sensitive information as much as possible with current statistics, we defined following $\chi^2$ for the neutrino oscillation analysis.

$$\chi^2 = \min_{\alpha_{^8B,hep}}^{\epsilon_{exp,theo}} \left[ \sum_{i=D,N}^{j=1,18} \left\{ \frac{\phi_{ij} - \phi_{ij}^{osci}(\alpha_{^8B}, \alpha_{hep}) \times f_j(\epsilon_{exp}, \epsilon_{theo})}{\sqrt{\sigma_{stat,ij}^2 + \sigma_{uncorr.sys,ij}^2}} \right\}^2 + \left( \frac{\epsilon_{exp}}{\sigma_{exp}} \right)^2 + \left( \frac{\epsilon_{theo}}{\sigma_{theo}} \right)^2 \right]$$

Then, the $\chi^2_{min}$ was obtained as 47.0 at $(0.80, 4.3 \times 10^{-10} eV^2)$ and the $\chi^2$ for the flat

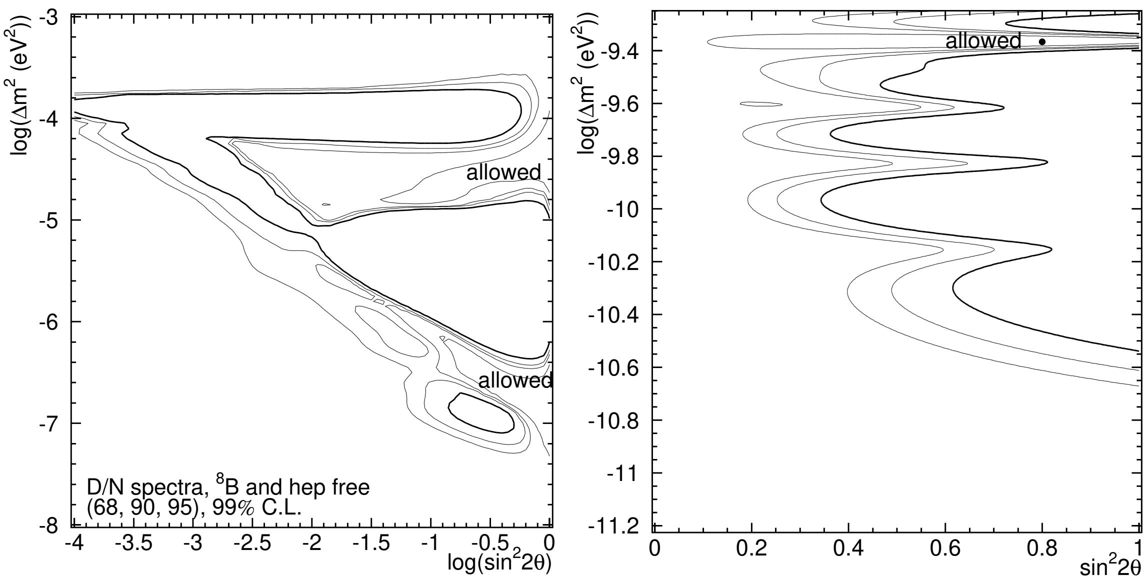


Figure 5: Excluded region from the day and night spectra are shown. Both $^8B$ and hep flux were treated as free parameter.

was 49.9 with 14 hep. The exclusion region obtained from the analysis is shown in the figure 5. Since we treated both $^8B$ and hep flux as free parameter, this analysis is independent of the absolute flux uncertainties of the SSMs and even high energy bins which have larger systematic errors are ineffective to results. Although we tried to omit high energy 4 bins, the excluded region didn't change a lot. Excluded region around SMA solution is expanding as accumulating statistics and a definite discrimination of SMA will be achieved in near future.

## 5. Seasonal variation

If the justso solution is the real solution, we expect a seasonal variation in wide parameter region. We divided data into 8 seasons and looked for a possible variation due to the neutrino oscillation. Observed seasonal variation with the data above 6.5 MeV and above 11.5 MeV are shown in the figure 6. In the figure, also shown are the expected variations only from the eccentricity (thin) and from the oscillation with parameter $(1, 4.29 \times 10^{-10} eV^2)$ (thick). As shown in the figure, expected seasonal variation can be enhanced by raising the energy threshold with this parameter. The $\chi^2$ values of the seasonal variation with arbitral normalization are 2.0, 2.5 and 8.0 for no oscillation, with oscillation and flat, respectively. SK sees seasonal variation due to the eccentricity, but no oscillation effect in the data integrated above 6.5 MeV. However, $\chi^2$ values with the data above 11.5 MeV are 6.7 and 4.7 for no oscillation and with oscillation and oscillation gives slightly better fit. It may be a hint of a justso solution, but we need much more (probably more than 5 years) statistics in order to distinguish the oscillation from no oscillation by a seasonal variation information.

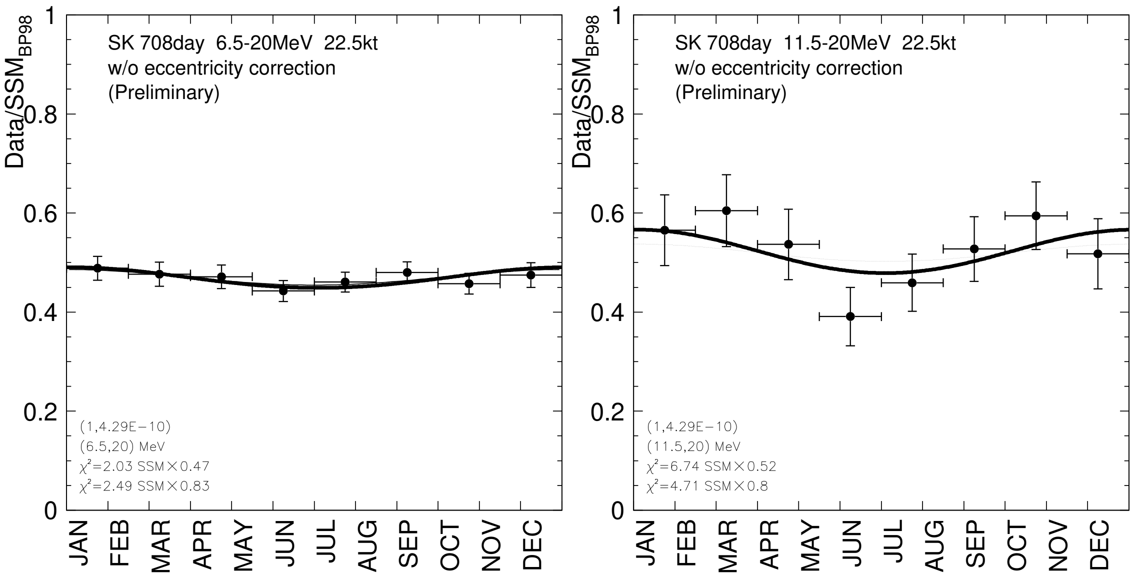


Figure 6: Left: Observed seasonal variation with the data above 6.5 MeV is shown with the expected variation due to the eccentricity (thin) and an oscillation $(1, 4.29 \times 10^{-10} eV^2)$ (thick). Right: Observed seasonal variation with the data above 11.5 MeV is shown.

## 6. Global analysis

Finally, we performed a global analysis which contains SK day and night spectra, Homestake flux result and SAGE and Gallex flux results. This global analysis was done by adding $\chi^2$ values obtained in figure 2 and in figure 5. Obtained results are shown in figure 7. Because the preferred region by SK spectrum and that by global flux analysis don't overlap well, allowed region in the justso region is very weak. And local $\chi^2$ minimums in each allowed islands are obtained as 52.7, 53.8, 54.9, 58.6 and 59.6 for LMA $(0.79, 3.5 \times 10^{-5} eV^2)$, SMA $(6.3 \times 10^{-3}, 5.0 \times 10^{-6} eV^2)$, LOW $(0.89, 1.1 \times 10^{-7} eV^2)$, justso1 $(0.89, 4.4 \times 10^{-10} eV^2)$ and justso2 $(0.70, 6.5 \times 10^{-11} eV^2)$, respectively. We found the minimum value at the LMA solution region with this most informative analysis and the best fit was met with 34 times hep flux than the SSM. The $\chi^2$ value for the no oscillation was 111.9 and again neutrino oscillations are strongly favored by the experimental results.

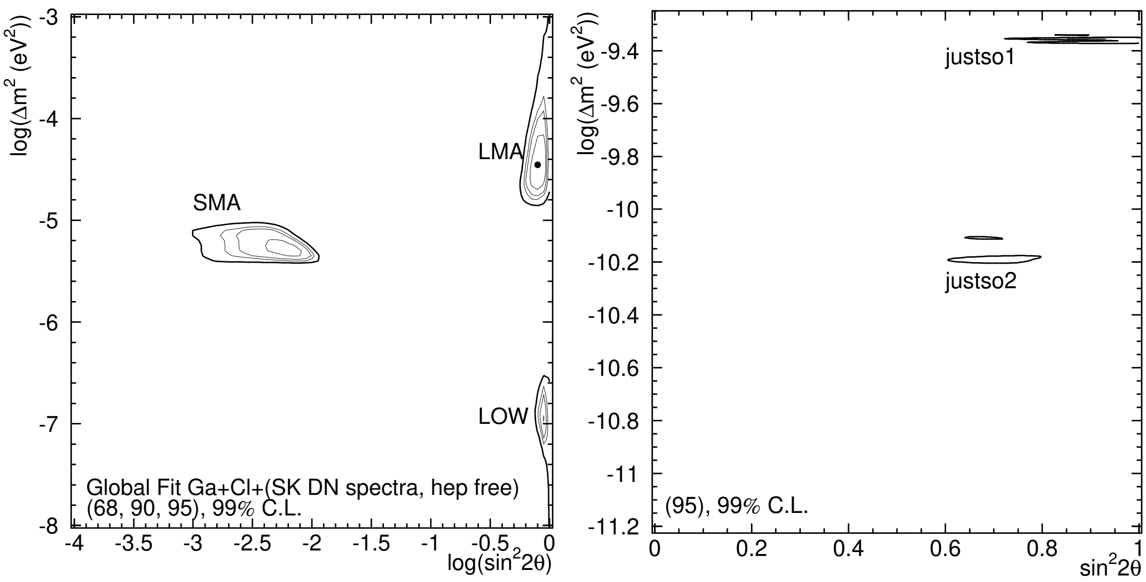


Figure 7: Allowed region from the global analysis. Homestake, SAGE, Gallex and SK day and night spectra results are used. The best fit parameter is shown by a dot.

## 7. Summary

SK has updated the results with 708 days data. No significant but small DN asymmetry was seen. Due to the small DN asymmetry, $\chi^2_{min}$ of DN analysis was found near the LMA solution. Notably, the analysis threshold was lowered to 5.5 MeV by a SLE trigger. Due to this low analysis threshold, SK has gained a discrimination power of spectrum distortion and small mixing angle solution seems to be giving bad fit in energy spectrum. The obtained spectrum is flat in low energy side and has slope (but not very significant) in high energy side. Justso solution can give very good fit to the spectrum but also large hep flux can reproduce the slope. In order to distinguish the justso solution, seasonal variation in high energy events will be useful, but we need much more statistics for the study. All combined global analysis gives best fit parameter at the LMA region, but all the LMA, SMA and LOW solutions are allowed at similar confidence level. Solar neutrino results are not conclusive yet. However, SK is is certainly reaching the level of statistics and sensitivity to distinguish various oscillation solutions and will provide conclusive results in near future.

## 8. References


1) S.P.Mikheyev and A.Y.Smirnov, Sov. Jour. Nucl. Phys. **42**, 913 (1985); L.Wolfenstein, Phys. Rev. D**17**, 2369 (1978).
2) L.Glashow and L.M.Krauss, Phys. Lett. **B190**, 199 (1987).
3) Y.Fukuda et al., Phys. Rev. Lett. **81**, 1158 (1998).
4) Y.Fukuda et al., Phys. Rev. Lett. **82**, 1810 (1999).
5) Y.Fukuda et al., Phys. Rev. Lett. **82**, 2430 (1999).
6) Y.Fukuda et al., Phys. Rev. Lett. **77**, 1683 (1996).
7) M.Nakahata et al, Nucl. Instr. Meth. A421, 113 (1999).
8) J.N.Bahcall et al., astro-ph/9805135.
9) A.S.Brun, S.Turck-Chièze and P.Morel, astro-ph/9806272.
10) B.T.Cleveland et al., Astrophys. J. **496**, 505 (1998).
11) J.N.Abdurashitov et al., Phys. Lett. B**328**, 234 (1994); V.Gavrin et al., in *Neutrino 98*, Proceedings of the XVIII International Conference on Neutrino Physics and Astrophysics, Takayama, Japan, 4-9 June 1998, edited by Y.Suzuki and Y.Totsuka. To be published in Nucl. Phys. B (Proc. Suppl.);
12) P.Anselmann et al., Phys. Lett. B**342**, 440 (1995); W.Hampel et al., Phys. Lett. B**388**, 364 (1996); T.Kirsten et al., in *Neutrino 98*.
13) G.L.Fogli and E.Lisi, Astrop. Phys. **3**, 185 (1995).
14) J.N.Bahcall and M.Pinsonneault, Rev. Mod. Phys. **67**, 781 (1995).
15) J.N.Bahcall et al., Phys. Rev. C**54**, 411 (1996).
16) J.N.Bahcall, Phys. Rev. C**56**, 3391 (1997).
17) A.M.Dziewonski and D.L.Anderson, Phys. Earth Planet. Inter. **25**, 297 (1981).
18) J.N.Bahcall and P.I.Krastev, Phys. Rev. C**56**, 2839 (1997).
19) J.N.Bahcall et al., Phys. Rev. C**54**, 411 (1996).